Spherical polyelectrolyte brushes in the presence of multivalent counterions: The effect of fluctuations and correlations as determined by molecular dynamics simulations

Yu Mei,[1] Martin Hoffmann,[1] Matthias Ballauff,[1] and Arben Jusufi[1,2,*]
[1]*Physikalische Chemie I, University of Bayreuth, 95440 Bayreuth, Germany*
[2]*Department of Chemical Engineering, Princeton University, Princeton, New Jersey 08544, USA*
(Received 21 May 2007; revised manuscript received 14 August 2007; published 20 March 2008)

We consider the interaction of multivalent counterions with spherical polyelectrolyte brushes (SPBs). SPBs result if linear polyelectrolyte chains (contour length 60 nm) are densely grafted to colloidal spheres of 116 nm in diameter. When dispersed in water the surface layer, consisting of chains of the strong polyelectrolyte poly(styrene sulfonic acid), will swell. Recent work [Mei *et al.*, Phys. Rev. Lett. **97**, 158301 (2006)] has demonstrated that spherical polyelectrolyte brushes undergo a collapse in the presence of a mixture of monovalent and multivalent counterions. The collapse crossover could be well described by a mean-field approach. Here we demonstrate that the application of a mean-field approach is well founded by simulation results done with molecular dynamics (MD). MD simulations show that over a wide range of multivalent counterion concentration the effects of ion correlation and fluctuations can be neglected. Higher-valent counterions are shown to interact strongly with the polyelectrolyte chains of the SPBs and thus exhibit a much reduced osmotic activity in the system. This reduction is the driving force for the collapse.

DOI: 10.1103/PhysRevE.77.031805 PACS number(s): 82.35.Rs, 82.35.Gh, 82.39.Wj, 82.70.−y

I. INTRODUCTION

Polyelectrolyte brushes are systems in which polyelectrolyte chains are attached densely to a planar or curved surface. The term brush denotes a system in which the grafting density σ as expressed by the number of grafted chains per unit area is high enough so that neighboring chains strongly interact and are stretched away from the surface. Attaching long polyelectrolyte chains to colloidal core particles leads to spherical polyelectrolyte brushes (SPBs) as shown schematically in Fig. 1 [1–4]. The main feature of polyelectrolyte brushes is the strong confinement of the counterions within the brush layer first predicted by Pincus as well as Birshtein, Borisov, and Zhulina [5,6]. If monovalent counterions are present, the high number of charges present in such a polyelectrolyte brush will therefore lead to a strong stretching of the attached chains in order to alleviate the concomitant osmotic pressure of the counterions. This prediction is in full agreement with all experimental data available so far in planar systems [7–16] as well as in strongly curved polyelectrolyte brushes [2,3,17,18]. A recent review of these investigations was presented in Ref. [4]. By now, polyelectrolyte brushes in the presence of monovalent counterions may be regarded as rather well-understood systems.

A major point of interest is the investigation of collapse transitions in polyelectrolyte systems. Up to now, theoretical investigations of density profiles in planar polyelectrolyte brushes have been done by considering possible phase transitions within the brush layer and their dependence on solvent quality and grafting density [6,19–23]. However, much less attention has been paid to the interaction of polyelectrolyte brushes with multivalent counterions. Within the framework of mean-field theories, a weak swelling of the brush layer was predicted [24]. More recently, Santangelo and Lau have calculated counterion fluctuation effects on planar polyelectrolyte brushes [25]. They predicted that fluctuation terms may lead to a collapse transition of the brush height with increasing ion valency. A recent experimental investigation of the interaction of spherical polyelectrolyte brushes with trivalent counterions done in our group clearly demonstrated that a mean-field approach is capable of describing the swelling of the brush in a nearly quantitative fashion [26]. As argued in Ref. [26], the trivalent counterions are strongly correlated with the polyelectrolyte chains of the brush layer. Thus, they may be regarded as fully condensed to the polyelectrolyte chains and do not contribute to the osmotic pressure within the layer. Initial molecular dynamics (MD) simulations presented there indeed pointed to a much reduced mobility of the trivalent ions as compared to the monovalent counterions. However, a clear proof of this conjecture could not yet be given.

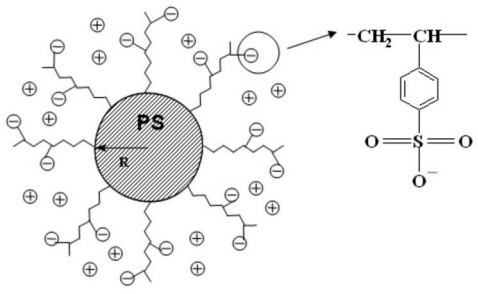

FIG. 1. Schematic representation of the spherical polyelectrolyte brush investigated in this study. Anionic polyelectrolyte chains are grafted to colloidal particles (radius R) made from solid polystyrene. The particles are immersed in aqueous salt solutions with defined ionic strength. The thickness L of the brush layer is measured for different ionic strengths by dynamic light scattering. The ionic strength in the system is adjusted through the concentration c_a of added salt. The equilibrium concentration c_s of salt within the brush layer can be treated in terms of a Donnan equilibrium.

*ajusufi@princeton.edu

Here we present a comprehensive investigation of spherical polyelectrolytes in the presence of multivalent counterions. We compare results of data obtained from MD simulations to recent experimental data [26]. From a detailed analysis of the MD results, it will become apparent that multivalent counterions exhibit a much more pronounced interaction with the polyelectrolyte chains than monovalent ions. MD simulations will furthermore allow us to discuss the effects of fluctuations within the system. In this way the applicability of the mean-field approach applied in Ref. [26] can be discussed in detail.

The paper is organized as follows. In Sec. II we briefly outline the main experimental findings related to the collapse of spherical polyelectrolyte brushes in the presence of trivalent ions. Special emphasis is laid on possible experimental problems that may disturb these measurements. Section III discusses these findings in terms of a mean-field approach while Sec. IV is devoted to the MD simulations of these systems in the presence of counterions in a valency range from 1 to 4. Most notably, we shall discuss the effects of correlations and fluctuations on spherical polyelectrolyte brushes. The brief Sec. V concludes this paper.

II. SPHERICAL POLYELECTROLYTE BRUSHES IN PRESENCE OF TRIVALENT COUNTERIONS: DYNAMIC LIGHT SCATTERING

The spherical polyelectrolyte brushes were synthesized using the method devised previously [1]. The systems investigated here are quenched spherical polyelectrolyte brushes carrying chains of the strong polyelectrolyte poly(styrene sulfonic acid). When dispersed in water the surface layer consisting of such a polyelectrolyte brush will swell. The core particles are practically monodisperse (cryo transmission electron microscopy gives $r=56\pm2$ nm) and the hydrodynamic radius R_H determined by dynamic light scattering (DLS) is related to the brush height L through $R_H=R+L$ where R denotes the radius of the core particles. All systems investigated here have been fully characterized in Millipore water with regard to their structural parameters, namely, the contour length $L_c=60$ nm of the grafted chains, the radius $R=58$ nm of the core particles, the mass per particle $m_P=1.07\times10^{-15}$ g, and the grafting density $\sigma=0.064$ nm^{-2} giving the number of chains per unit area.

Dynamic light scattering was done using a Peters ALV 4000 light scattering goniometer. A small amount (10 μl) of a given suspension of the SPBs (solid content 1.43%) was added to the respective salt solution to a particle concentration of 55 ppm. The change of the salt concentration caused by adding the SPBs can hence be neglected. This problem has been checked in separate experiments [26]. The suspension are transferred into clean tubes made of quartz and the DLS measurements were conducted mostly at an angle of 90°. In some cases measurements have been done using different scattering angles (30°–150°). The correlation function was checked in all cases to exclude possible disturbance by the onset of aggregation. The thickness L of the brush layer is calculated from the hydrodynamic radius R_H through $L=R_H-R$.

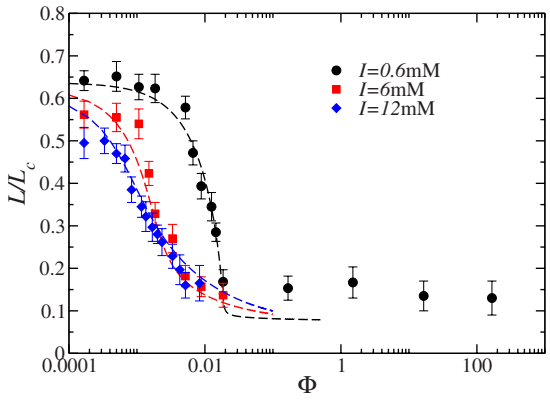

FIG. 2. (Color online) Relative brush thickness L/L_c in presence of a mixture of monovalent (Na^+) and trivalent (La^{3+}) counterions vs ion concentration ratio $\Phi=c_{La^{3+}}/c_{Na^+}$. Parameter of the different sets of data is the overall ionic strength I. The lines are theoretical calculations obtained from mean-field theory; see Sec. III for further details. This figure is taken from our previous work [26].

Dynamic light scattering was done at very high dilution, corresponding to volume fractions below 10^{-4}. It thus gives the brush thickness L in the limit of infinite dilution. Possible disturbances by mutual interaction between different particles can be excluded. Moreover, electroviscous effects modifying the diffusion coefficient are of negligible importance. Hence, DLS gives direct access to L for various salt concentrations. Since we are dealing with a quenched brush in all cases to be discussed here, the pH in the system does not influence L [2]. The thickness L thus obtained can be directly compared to data obtained for the thickness of planar brushes.

As mentioned above, full replacement of the monovalent counterions of the particles by the trivalent La^{3+} ions leads to immediate flocculation unless the ionic strength is below $10^{-4}M$. Hence, we immersed the particles in mixtures of salt solutions containing La^{3+} and Na^+ ions in a given ratio.

Figure 2 shows the relative thickness L/L_c of the brush layer of the quenched SPB in the presence of trivalent La^{3+} counterions, taken from our previous work [26]. The parameter I is the overall ionic strength of added salt. At first a marked shrinking is observed, which is most pronounced for an ion concentration ratio $\Phi=c_{La^{3+}}/c_{Na^+}\gtrsim0.001$, depending on the ionic strength I. For low concentration ratio Φ, the suspension remains stable, but higher Φ is followed by coagulation of the particles for $I>0.006M$. The coagulation of the particles points to an effective attraction between the particles. Recently, Tirrell and co-workers demonstrated that multivalent ions lead to attraction between planar polyelectrolyte brushes [27]. The strong shrinking of the brush layer upon addition of trivalent counterions must first be traced back to the enormous lowering of the osmotic pressure within the brush layer. On average, three monovalent counterions are replaced by one La^{3+} ion, thus reducing the osmotic pressure by a factor of about 3. In addition, the strong binding of the multivalent ions to the polyelectrolyte chains leads to further decrease of the osmotic pressure. In the following, the various aspects of the theoretical treatment of these experimental findings are discussed.

III. MEAN-FIELD THEORY OF SPB COLLAPSE

We begin with the case of a single SPB in the presence of a mixture of mono- and multivalent counterions without added salt. Although a simplification, we assume that the SPB is completely neutralized by its counterions, i.e., the vast majority of the counterions are captured inside the SPB. This is justified as long as the SPB is highly charged. In fact, experimental studies has proven that more than 95% of the counterions are located inside the highly charged brush [17], depending on the grafting density σ.

Based on the arguments of Alexander and de Gennes the brush size can be determined by balancing the forces of the polyelectrolyte chains by the osmotic pressure forces from the trapped counterions [24,28,29]. The chain forces consist of an elastic part and an excluded volume Flory-type contribution, yielding a total chain force F_{ch}

$$F_{\mathrm{ch}} = -\frac{3kTfL}{Na^2} + v_0 kT(fN)^2 \frac{9(R+L)^2}{8\pi[(R+L)^3 - R^3]^2}. \quad (1)$$

The parameters are the chain number $f=4\pi\sigma R^2$, with R being the core radius, the degree of polymerization N, and the excluded volume parameter $v_0 \approx a^3$. The monomer size a is around 0.25 nm [30,31] and kT is the thermal energy. The brush thickness can be calculated by balancing the chain force with the osmotic pressure forces that arise from the confined counterions. In a mixture of multi- and monovalent counterions, the osmotic pressure force inside the brush is given by

$$F_p^i = kT(c_+^i + c_{q+}^i)4\pi(R+L)^2, \quad (2)$$

where c_+^i is the concentration of monovalent counterions inside the brush and c_{q+}^i that of the multivalent ones with valency q. The concentrations are number densities N_x/V_{in}, with N_x being the number of counterions of species x ($x=+,q+$) and $V_{\mathrm{in}}=(4\pi/3)[(R+L)^3-R^3]$ being the brush volume. According to the experimental system we consider without loss of generality the case that the SPB is negatively charged and the counterions positively charged. We used here only the ideal gas contribution to the osmotic pressure. We shall investigate in Sec. IV the importance of virial contributions to the osmotic pressure. Balancing Eqs. (1) and (2) yields the brush thickness L. The variables are c_+^i and c_{q+}^i. Using the neutralization condition $qc_{q+}^i + c_+^i = c_m$, with $c_m = fN/V_{\mathrm{in}}$ being the charged monomer concentration inside the brush, it is possible to calculate the brush thickness as a function of the ion ratio $\Phi = c_{q+}/c_+$, with c_{q+} and c_+ denoting the overall ion concentrations in the SPB solution. We will compare this approach with simulation results in the next section.

We now consider the case where salt is added to the system. There are only the ideal osmotic pressure terms of the added salt ions that have to be accounted for. The remaining osmotic pressure force F_p is now:

$$F_p = \Delta\Pi 4\pi(R+L)^2, \quad (3)$$

with the ideal osmotic pressure difference $\Delta\Pi = kT\Sigma_{x=q+,+,-}(c_x^i - c_x^o)$; the concentrations c_x^o are the ion concentrations outside of the brush. Again, the brush thickness L is obtained by the force balance $F_{\mathrm{ch}}=F_p$. However, there are now six dependent variables, namely, c_x^i and c_x^o ($x=q+,+,-$). We solve the problem by taking into account the Donnan equilibrium, which is

$$\frac{c_{q+}^i}{c_{q+}^o} = \left(\frac{c_+^i}{c_+^o}\right)^q = \left(\frac{c_-^o}{c_-^i}\right)^q. \quad (4)$$

The neutralization conditions inside and outside the brushes are

$$qc_{q+}^i + c_+^i = c_m + c_-^i, \quad (5)$$

$$qc_{q+}^o + c_+^o = c_-^o. \quad (6)$$

If the ionic strength $I=(1/2)\Sigma_{x=q+,+,-}q_x^2 c_x$ is fixed, the brush thickness L can be calculated with respect to a given concentration ratio $\Phi = c_{q+}/c_+$. Note that Eqs. (1) and (3)–(6) have to be solved simultaneously.

A few remarks should be made regarding Eq. (4). The ratios stem from the condition that at equilibrium the difference of the chemical potentials inside and outside the brush of each ion component vanishes; see the Appendix. It should also be noted that only the ideal gas contributions of the chemical potentials remain. Electrostatic contributions treated in a mean-field fashion cancel one another out if the density distributions of each ion species possess the same profile.

We now apply the theoretical approach, namely, the calculation of the brush thickness from Eqs. (1) and (3) to the experimental data presented in previous work [26]. Here we take advantage of the Donnan equilibrium (4) together with Eqs. (5) and (6). Figure 2 displays the comparison of theory and experiment. Evidently, the mean-field approach captures all of the salient features of the experimental data: At a low ratio Φ, the reduced thickness L/L_c of the brush stays practically constant. In this regime the height of the brush is therefore determined only by the ionic strength in the system. At higher Φ, the reduced thickness decreases drastically until a constant value is reached. Obviously, strong ion exchange has led to an enrichment of the trivalent ions at the expense of the monovalent counterions as shown in previous work [26]. The mean-field approach expounded in this section describes the ratio Φ at which the collapse starts, as well as the fact that L/L_c of the brush coincides with the final stage for all ionic strengths used in the experiments. Given the various sources of experimental error as well as the simplifications of the theory, the agreement of theory and experiment can be considered quantitative. Moreover, the collapse of the brush layer is not brought about by a phase transition but only by a strong reduction of the osmotic pressure due to the replacement of monovalent by trivalent counterions. The next section will explain this unexpected result by discussing detailed MD simulations of this system.

IV. MD SIMULATION OF A SINGLE SPB

A. Simulation model

The simulation model is analogous to the one used for simulating polyelectrolyte (PE) stars [32,33]. Csajka *et al.*

used a similar model for simulations of planar polyelectrolyte brushes with monovalent counterions [22]. We set similar values for the grafting density σ and charge fraction α. The brush is located in the center of a cubic box of edge length l. The chains that are grafted on the core surface are initially free to move (first 120 000 time steps) on the surface of the core particle, which is kept fixed at the central position. Thereafter the positions of the grafting monomers are kept fixed during the adjacent simulation runs. We used a time step of 0.002τ, with $\tau=\sqrt{ma^2/\varepsilon}$ being the time scale. The mass m and the diameter a of the counterions are the same as for the monomers. There is no added salt in this model system. ε is the Lennard-Jones energy scale (see Refs. [32,33]). The box edge was kept at $l=160a$, the number of chains was set to $f=40$, and the radius of the hard core is $R=6a$, yielding a grafting density $\sigma a^2=0.068$. The degree of polymerization is $N=30$ and that of ionization $\alpha=1.0$, representing full charging, which yields a SPB bare charge of $1200|e|$; e is the elementary charge. The temperature was held at the desired value of $T=1.2\varepsilon/k$ using a stochastic method according to the Langevin equation [22,32]. The Coulomb interactions are calculated using the Lekner technique [34,35], where the Bjerrum length was set to $3a$, corresponding to a value in water of 7.1 Å. All other parameters are the same as reported in Refs. [32,33].

After an equilibration run of 500 000 time steps we calculated all desired quantities for further 250 000 time steps (500τ). We extended the production run to 2500τ for cases with only one type of counterion ($c_{q+}=0\Leftrightarrow\Phi=0$ or $c_+=0\Leftrightarrow\Phi\to\infty$) and with equal amounts of them ($c_{q+}=c_+\Leftrightarrow\Phi=1$) with $q=1$–4. We observed that our measured quantities deviate weakly from the short-run results, e.g., the largest deviation of the brush thickness is around 8%; for most cases we obtained discrepancies of less than 1%. With a production time of 500τ or 2500τ we exceed the relaxation time. This quantity is obtained from the autocorrelation function (ACF) of the fluctuations of the radius of gyration R_g of the whole brush, given by $C(t)=\langle dR_g(t)dR_g(0)\rangle$, with t being the time. The fluctuations are defined as $dR_g(t)=R_g(t)-\langle R_g\rangle$ and $dR_g(0)=R_g(0)-\langle R_g\rangle$ [22,36]. The normalized ACF is plotted in Fig. 3 for different counterion valencies. $C(t)$ decays very fast, almost irrespective of the valency of counterions. From $C(t)$ one can extract a relaxation time $\tau_r=\int_0^{t_m}C(t)dt/[1-C(t_m)]$, with t_m being the length of the time intervals for the measurement of $C(t)$. The computed values of τ_r are given in the legend of Fig. 3. They range between 15τ and 18τ, and do not depend on the ion ratio Φ. The values of the relaxation time of spherical brushes are very similar to the values observed for planar brushes, which has been shown to be around 14τ at approximately the same grafting density [22]. The relaxation time of brushes is much shorter than for linear chain, in analogy to findings for star polymers, where the relaxation time scales with $f^{-0.5}$, faster than linear chains in a good solvent [37].

B. Collapse of SPB

We present results obtained from MD simulations of SPBs regarding the collapse of the brush layer at different ion concentration ratios Φ. We observe within this parameter range, for the case of the presence of monovalent counterions only ($\Phi=0$), an osmotic brush, in agreement with recent works [31,38,39]. Keeping the whole system charge neutral, we studied the following SPBs in the presence of a mixture of monovalent and di-, tri-, and tetravalent counterions at various concentration ratios Φ. No additional salt ions are included in the simulation system.

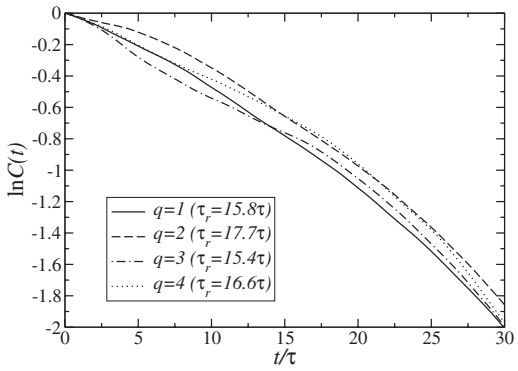

FIG. 3. Normalized autocorrelation function $C(t)$ of the radius of gyration R_g of the SPB vs time t. Shown are results from SPBs in the presence of only one type of counterion with valencies between $q=1$ and 4. The corresponding relaxation times τ_r are given in the legend.

We present results for the change in the center-to-end distance of the SPB if monovalent ions are partially exchanged by multivalent ions according to a given ratio Φ. Figure 4 shows two snapshots of a brush and gives a first impression of the effects occurring if the ratio between monovalent and trivalent counterions is unity ($\Phi=1$). The trivalent ions are almost completely confined within the brush, whereas a fraction, although small, of monovalent ones is also outside the brush. The upper snapshot shows also the polyelectrolyte chains in a coiled configuration. No stretching can be observed any longer in contrast to the case $\Phi=0$. As mentioned above, this is due to a weaker osmotic pressure.

We also observe that the trivalent ions are closely packed on the surface of the colloidal core, as can be seen from Fig. 4. In Fig. 5 we plot the radial charge distribution obtained from the difference of the monomer density distribution ρ_m and that of the counterions ρ_{q+}: $\rho_m(r)-q\rho_{q+}(r)$. Shown are cases at which only one type of counterion is present, i.e., $\Phi\to 0$ for $q=1$, and $\Phi\to\infty$ for $q>1$. Apart from modulation in the dense core region due to packing arrangements of the particles, the brush is completely neutralized by the counterions due to their correlation with the chains. This is the case for $q>1$ in particular. We will quantify these correlations in the next section in more detail. Here we shall focus on the collapse transition of the brush with varying Φ. For this purpose we computed the center-to-end distance R_{ce} of the terminal monomers located at $\mathbf{r}_i^t$, which is given by $R_{ce}^2=\frac{1}{f}\Sigma_{i=1}^f(\mathbf{r}_i^t-\mathbf{R}_{c.m.})^2$; $\mathbf{R}_{c.m.}$ denotes the position of the center of mass of the SPB. In Fig. 6 we show the brush thickness L as calculated from $\sqrt{\langle(R_{ce}-R)^2\rangle}$. We normalized L to the contour length L_c.

The theoretical calculations are in good agreement with simulation results for the trivalent ($q=3$) and tetravalent (q

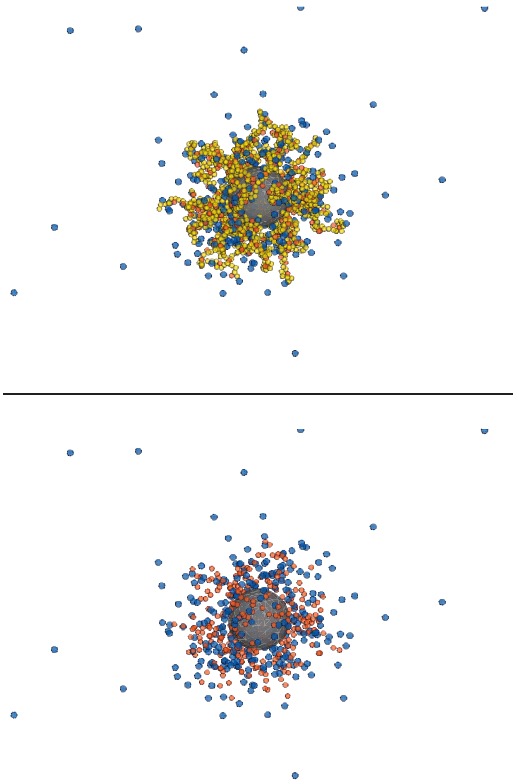

FIG. 4. (Color) Snapshots of SPB obtained from MD simulation. In both pictures monovalent (blue spheres) and trivalent (red spheres) counterions are shown. The upper picture shows the polyelectrolyte chains, represented by yellow colored spherical monomers, which are grafted with one end on the surface of the colloidal core particle (big gray sphere in the center). The lower picture is shown without the chains. The multivalent counterions are fully within the brush whereas the monovalent ions are partially outside.

=4) cases. The theoretical results are obtained by minimizing Eqs. (2) and (1). It is assumed that multivalent ions do not contribute to the osmotic pressure $\Delta\Pi$ in Eq. (3). This is due to the strong electrostatic binding of the ions to the chains. The contribution of monovalent counterions to the osmotic

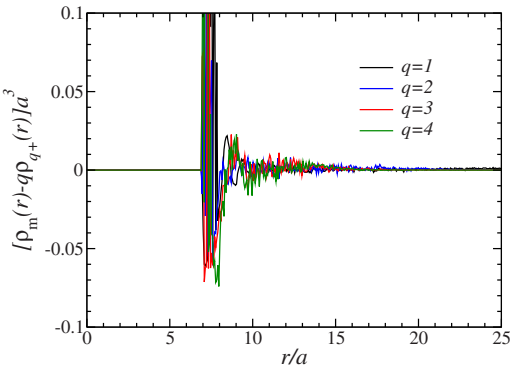

FIG. 5. (Color online) Radial charge density of the SPB. The core radius is $6a$ and the overall radius of the brush at $q=1$ is around $22a$, for $q=2$ around $17.1a$, and for $q\geq 3$ the overall radius is around $12a$.

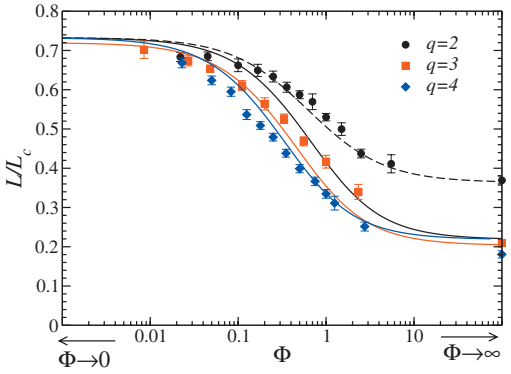

FIG. 6. (Color) Relative brush thickness L/L_c versus the ion concentration ratio Φ. Shown are simulation results of SPB with monovalent and multivalent counterions at various valencies q (symbols). The theoretical calculations are also shown, once with the assumption that the multivalent counterions are not osmotically active (solid lines), and once, for the divalent case, with a partial osmotic contribution (dashed line). The limits at $\Phi\rightarrow 0$ and $\Phi\rightarrow\infty$ represent cases at which solely monovalent and solely multivalent counterions are present, respectively.

pressure is 80% of the confined monovalent ions; around 90% of all monovalent counterions are confined according to simulation results for the case of no added multivalent ions ($\Phi=0$). The portion of ions that contribute to the osmotic pressure is in line with recent reported experimental results [26]. We keep this fit parameter constant for all Φ. However, for the divalent case it is observed that the assumption that those counterions do not contribute to the osmotic pressure leads to poor description of the simulation results. Obviously the divalent ions are not as strongly bound to the chains as ions with higher valency. Hence, a significant number of divalent ions possess translational entropic contributions. A best fit with the simulation results is obtained if one assumes that 1/3 of all divalent ions are osmotically active (dashed line in Fig. 6).

We stress that the assumption that the multivalent counterions possess no or only partial osmotic activity is in line with the theoretical treatment of the Donnan equilibrium (4). Since the ions are strongly bound to the chains their entropy is implicitly accounted for with the monomer chains, i.e., they move with the monomer chains. This is analogous to the osmotic pressure occurring in polymer solutions: The osmotic pressure of the polymer solution is directly related to the polymer density and not to the monomer density.

Since the simulation system does not contain additional salt ions, the collapse range of Φ in Fig. 6 is different from the range of the real systems shown in Fig. 2. In the experimental system Φ is given by the ratio of all multi- and monovalent ions, i.e., counterions from the SPB and from the salt. A direct comparison between the results of the simulation model and those of the experiment can be achieved by considering the relative brush thickness with respect to the ratio of confined ions, $\Phi^i=c^i_{q+}/c^i_+$. With the mean-field model we can calculate the amount of trapped ions according to the Donnan equilibrium and the neutralization conditions Eqs. (4)–(6), yielding Φ^i. For the salt-free case (model system), we set $c^i_{q+}=c_{q+}$ and $c^i_+=0.9c_+$, according to simulation re-

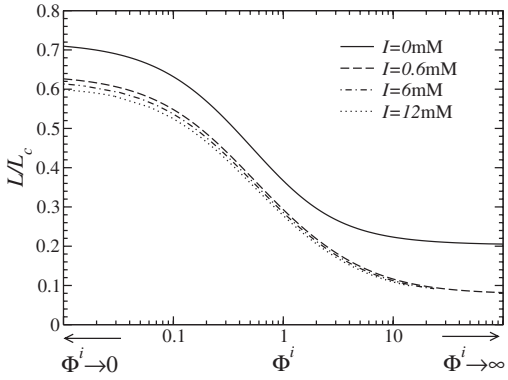

FIG. 7. Relative brush thickness L/L_c versus the concentration ratio Φ^i of the confined ions. Shown are theoretical results for the SPB with trivalent counterions ($q=3$) of the model system and the real system, the latter at various ionic strengths I. Note that the brush thickness also decreases with increasing ionic strength. The limits at $\Phi^i \to 0$ and $\Phi^i \to \infty$ represent cases at which solely monovalent and solely multivalent counterions are present, respectively.

sults. In Fig. 7, we plot the relative brush thickness L/L_c with respect to Φ^i for the model system (salt-free case with $q=3$), and for the experimental system (added salt, $q=3$) at different ionic strengths I. The plots show that the collapse transition of the salt-free system occurs in the same range of Φ^i as that of the experimental SPB with added salt. It clearly demonstrates that the concentration ratio of the confined ions is the seminal quantity for the brush extension. Note that the brush thickness also decreases with addition of salt due to the osmotic pressure from the (co)ions outside the brush. Evidently, the results of the MD simulations underscore the justification of applying a mean-field approach when discussing the experimental data shown in Fig. 2. In particular, MD simulations justify the assumption of neglecting the contribution of the trivalent ions in the calculation of the osmotic pressure within the brush layer. This central point will be discussed in further detail in the subsequent sections.

C. Correlation effects

We present a microscopic analysis of possible correlation and fluctuation effects. In our MD simulations various quantities are measured to obtain information about those effects. We start with the analysis of the osmotic pressure Π and its contributions. The osmotic pressure consists of ideal and virial contributions and is calculated via [22,40,41]

$$\Pi = kTc + W, \tag{7}$$

$$W = \frac{1}{3V}\left\langle \sum_{i=1}^{N_{\text{tot}}-1} \sum_{j=i+1}^{N_{\text{tot}}} \langle \mathbf{r}_{ij} \cdot \mathbf{F}_{ij}^s \rangle + \langle U_{\text{Coul}} \rangle \right\rangle. \tag{8}$$

The ideal term is directly related to the monomer and counterion densities $c=N_{\text{tot}}/V$, with N_{tot} being the total particle number in a volume V. We use the brush volume V_{in}, since the vast majority of all particles are within the brush. The remaining particles outside the brush, i.e., a small fraction of monovalent counterions, hardly possess significant entropic contribution to the brush pressure. The virial term W accounts for the pair interaction, namely, for the short-range forces $\mathbf{F}_{ij}^s$ on particle i due to j, along the interaction coordinate $\mathbf{r}_{ij}=\mathbf{r}_i-\mathbf{r}_j$. In our MD simulations these forces consist of the Lennard-Jones and finite extensible nonlinear elastic (FENE) forces between bonded monomers. In addition there is the electrostatic energy U_{Coul} which contributes to the virial term W.

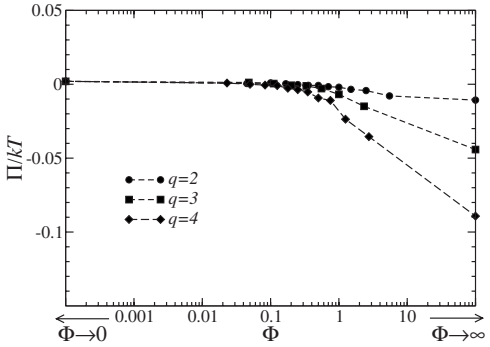

FIG. 8. Total osmotic pressure Π versus the ion concentration ratio Φ. Shown are simulation results of SPB with monovalent and multivalent counterions at various valencies q. The limits at $\Phi \to 0$ and $\Phi \to \infty$ represent the cases at which solely monovalent and solely multivalent counterions are present, respectively. The lines are guides for the eye.

In Fig. 8 the total osmotic pressure is shown as a function of Φ for the considered multivalent cases ($q=2,3,4$). It can be observed that until $\Phi \lesssim 1$ the total osmotic pressure is around 0, in particular if one takes into account the error bars, which are around $0.01kT$. However, for higher values of Φ, i.e., when the number of multivalent counterions exceeds that of the monovalent ones, a significant negative value of the total pressure is observed, although the absolute scale is quite small ($\lesssim 0.1kT$). Nevertheless, it is a significant trend that with increasing valency an unstable region occurs. This is in line with other observations made in polyelectrolyte networks. Let us look into more detail of the various virial contributions that cause this negative total pressure, similarly to the analysis of Yin *et al.* [41] applied to polyelectrolyte networks. For this purpose we further decompose the virial term W into the following contributions:

$$W = W_{\text{Coul}} + W_{\text{ion}}^s + W_{\text{chain}}^s, \tag{9}$$

$$W_{\text{Coul}} = \frac{1}{3N_{\text{tot}}}\langle U_{\text{Coul}} \rangle, \tag{10}$$

$$W_{\text{ion}}^s = \frac{1}{3N_{\text{tot}}}\left\langle \sum_{i=1}^{N_{\text{ion}}-1} \sum_{j=i+1}^{N_{\text{ion}}} \langle \mathbf{r}_{ij} \cdot \mathbf{F}_{ij}^s \rangle + \sum_{i=1}^{N_{\text{ion}}} \sum_{j=1}^{fN} \langle \mathbf{r}_{ij} \cdot \mathbf{F}_{ij}^s \rangle \right\rangle, \tag{11}$$

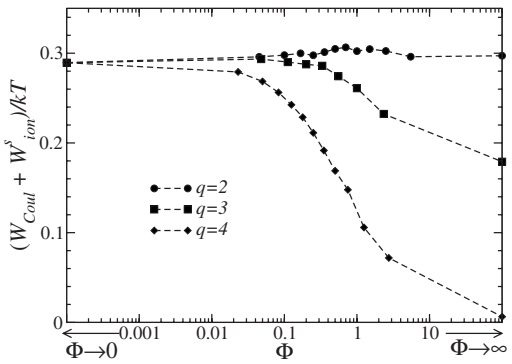

FIG. 9. Sum of virial pressure terms resulting from all electrostatic interactions W_{Coul} and from short-range forces acting on all counterions, denoted by W^s_{ion} as a function of the concentration ratio Φ. Shown are simulation results of SPBs with monovalent and multivalent counterions at various valencies q. The limits at $\Phi \to 0$ and $\Phi \to \infty$ represent the cases at which solely monovalent and solely multivalent counterions are present, respectively. The lines are guides for the eye.

$$W^s_{\mathrm{chains}} = \frac{1}{3N_{\mathrm{tot}}}\left\langle \sum_{i=1}^{fN-1} \sum_{j=i+1}^{fN} \langle \mathbf{r}_{ij} \cdot \mathbf{F}^s_{ij} \rangle \right\rangle. \tag{12}$$

Note that these contributions are calculated per particle, i.e., they are divided by the particle density c. The first term W_{Coul} consists of all electrostatic interactions, the second term W^s_{ion} is a sum of all short-range interactions, i.e., Lennard-Jones interactions, among counterions [first sum in Eq. (11)] and among counterions and monomers [second sum in Eq. (11)]. The last term W_{chains} takes into account the short-range interactions between monomers only, namely, the Lennard-Jones and FENE potentials.

As was already reported for the case of planar brushes and PE networks, the overall negative electrostatic virial term W_{Coul} is canceled by the positive short-range ion virial term W^s_{ion} [22,41]. Here we show the sum of both terms and observe qualitatively the same result; see Fig. 9. The electrostatic interactions are completely outmatched by the short-ranged excluded volume interaction of the counterions. The Lennard-Jones contribution measured between ions is very small, i.e., the second sum in Eq. (11) is vastly dominant. This points to an increasing condensation of the ions in general with increasing multivalent ion fraction. However, for higher valency electrostatic correlations become more important. Nevertheless, the Coulomb virial term W_{Coul} is still canceled by W^s_{ion}. This is in agreement with results of Csajka *et al.* [22] for the case of planar brushes with monovalent counterions, and the study of PE networks by Yin *et al.* [41], where the same effect was reported for trivalent counterions.

This means that the observed negative pressure in Fig. 8 stems from other contributions. The remaining third term in Eq. (9), W^s_{chains}, and the ideal contributions remain in our analysis. Since the latter is always positive the only negative contributions occurs in W_{chains}. In particular, the bond potential, expressed by the FENE term, is responsible for the negative virial contribution, as in the PE network study of Yin *et al.* [41] Obviously, the stiffness of the chains is reduced. Previous works have demonstrated that counterions that are strongly correlated with a chainlike macroion, such as DNA strands, can reduce their stiffness tremendously, reaching collapsed configurations [42–46]. However, we stress that the observed collapse is already completed at ion ratio $\Phi > 1$.

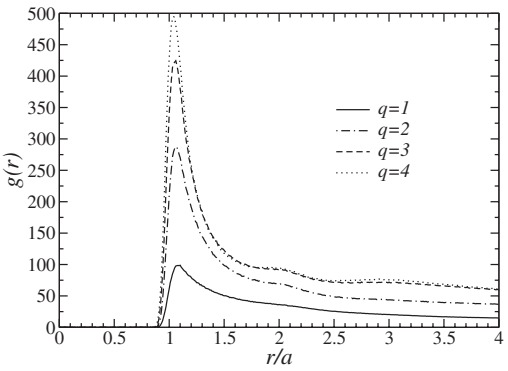

FIG. 10. Pair correlation function between monomers and counterions. Only systems with counterions of the same valency are shown, corresponding to $\Phi \to 0$ ($q=1$) or $\Phi \to \infty$ ($q=2,3,4$).

The decrease of the osmotic pressure due to higher electrostatic correlations corresponds to strong condensation. We verify this by showing monomer counterion pair correlation functions at limits where solely one type of counterions is present (see Fig. 10). As expected, the first correlation peak increases with increased valency, i.e., condensation becomes stronger. Note that the correlation peak is more than three times higher for multivalent ions than for monovalent ones. Also, with increasing valency a second peak arises. For the tri- and tetravalent cases a small third bump even occurs. Obviously more structure is established around each condensed ion. We conclude that strong condensation takes place for multivalent counterions. As we guessed in our previous work, only at high fraction of multivalent counterions $\Phi > 1$ do correlation effects become important. However, above this point the collapse is almost accomplished.

D. Ion mobility

One of the basic assumptions of our mean-field model is that multivalent counterions are not osmotically active. In the last section we showed that indeed multivalent counterions are much more strongly correlated with the chains than their monovalent counterparts.

As was shown in our previous work for the case of trivalent counterions, the mobility of the ions can help to verify the strong ion binding. In fact, we showed in Ref. [26] that the self-diffusion coefficient of the monovalent ions is almost six times higher than that of the multivalent ones at the same ratio ($\Phi = 1$). In Fig. 11 we present a comparison of the mean-square displacement (MSD) of all ions and monomers for cases where only one type of counterion is present. From the relation $\langle \Delta r^2 \rangle = 6D_0 t$, the self-diffusion coefficient D_0 can be obtained. Note that the time range shows linear-dependency behavior. For larger time scales a plateau is reached [22]; that is not shown here. The results of the MSD

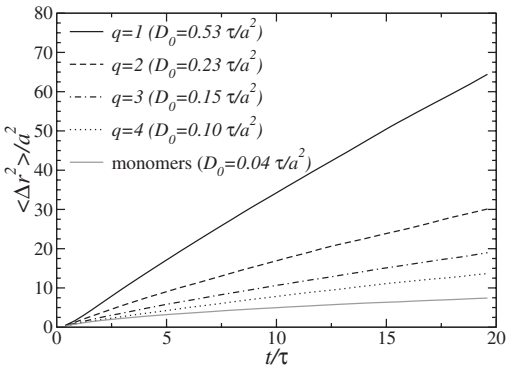

FIG. 11. Mean-square displacement of counterions and monomers. The self-diffusion coefficient is obtained from the slope of the lines above 7.5τ. Systems that contain only one counterion species are shown, corresponding to $\Phi \to 0$ $(q=1)$ or $\Phi \to \infty$ $(q>1)$.

data clearly indicate that the mobility decreases significantly with increasing ion valency. For comparison, the MSD of the chains is shown as well. Naturally, the monomers possess a small diffusion coefficient, due to the chain attachment to the core. However, in contrast to the monovalent ions, the tetra- and trivalent ions possess only a slightly higher diffusion coefficient.

We observe the same behavior also in the ion mixture. As an example, we take the case $\Phi=1$ and compare directly the MSD of the monovalent ion with that of the multivalent ones. This comparison was also done in our previous work, but only for the trivalent case [26]. Figure 12 shows for all cases $(q \geq 2)$ the MSD of the multivalent counterions and that of the monovalent ones. In order to quantify the significant difference of mobility of both ion species in the same brush, we introduce the ratio $\delta = D_0(q>1)/D_0(q=1)$. The values demonstrate the strong discrepancy in the mobilities. In addition, we observe minor changes in the MSD of the monomers or of the monovalent counterions, irrespective of the type of multivalent ion also present in the system. Therefore the change of δ is solely caused by the valency of the multivalent ions. We conclude that indeed there must be a

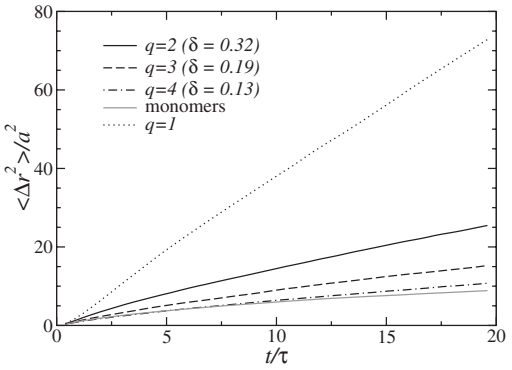

FIG. 12. Mean-square displacement of counterions for the case of equal amount ratios $(\Phi=1)$. Shown is the MSD of multivalent counterions (black curves) and that of monovalent ones in the same ion mixture (bright curve). δ is defined as the ratio of $D_0(q>1)/D_0(q=1)$. For comparison the MSD of the monomers is also shown.

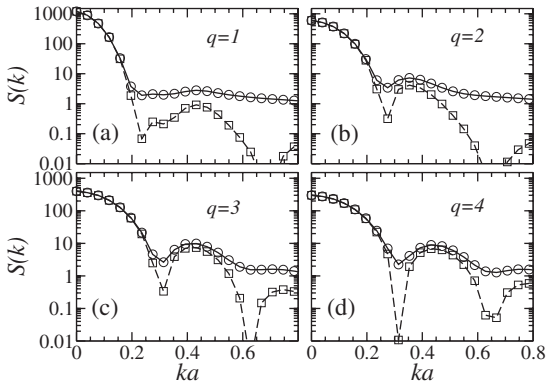

FIG. 13. Structure factor of counterions $S(k)$ at different valencies q. Only one type of counterion is present, corresponding to $\Phi=0 \Leftrightarrow q=1$ (a), and $\Phi \to \infty \Leftrightarrow q=2,3,4$ (b)–(d). Shown are the exact calculations $S(k) \sim \langle \hat{g}(k) \rangle$ (circles) and the mean-field approximations $S(k) \sim \langle \hat{\rho}(k) \rangle^2$ (quadrangles) [32,48]. Lines are guides for the eye.

strong correlation of the multivalent counterions. In contrast to polyelectrolyte networks, we also conclude from our MSD data that here there is hardly any mobility of the multivalent counterions, i.e., the translational contribution to the osmotic pressure is mainly determined by the monovalent counterions. Only the divalent counterions possess a relatively high mobility, which underlines their osmotic activity. That explains why our mean-field model requires a significant fraction of divalent ions—around 30% of ions which are osmotically active—in order to describe the simulation results for the size reduction properly (see the discussion of Fig. 6). Note that the reduced mobility of the multivalent counterions is not causing the reduction of the osmotic pressure. The argument is that strong ion-chain correlation of the multivalent ions leads to condensation and therefore to a smaller mobility. At the same time the same strong correlation reduces the osmotic pressure as well.

E. Fluctuation effects

We now analyze fluctuation effects of the counterions. A similar analysis was provided in the case of polyelectrolyte stars [32] with monovalent counterions. The principal idea is to compare the square of the averaged Fourier transform of the counterion density profile with respect to the center of the brush, $\hat{\rho}^2(k)$, with the Fourier transform of the correlation function among the counterions, $\hat{g}(k)$; k is the reciprocal coordinate. The average $\langle \hat{g}(k) \rangle \sim \langle \hat{\rho}^2(k) \rangle$ describes the structure factor $S(k)$ of the counterions. However, $\langle \hat{\rho}(k) \rangle^2$ is a mean-field approximation of $\langle \hat{g}(k) \rangle$. The latter is computed "on the fly" and provides an "exact" method to compute $S(k)$ in simulations. Details of the statistical mechanical justification of the structure factor calculations are described in Ref. [47], and recent applications can be found in Refs. [32,48]. Results of structure factor calculations shown here for cases where only one type of counterion is present $(\Phi=0, \Phi \to \infty)$ are summarized in Fig. 13.

It shows that with increasing valency the agreement between $\langle \hat{g}(k) \rangle$ and $\langle \hat{\rho}(k) \rangle^2$ becomes better, even at higher k

values. Note that, while the former quantity tends to unity the latter converges to zero as $k \to \infty$, i.e., they diverge at high k values [47,48]. At small k values ($ka < 0.2$), the two quantities agree. This proves that shape fluctuations are very weak and that the simulation times are much longer than the relaxation times. For bigger k values there are differences in the four cases shown. Since with increasing valencies the agreement between the two quantities becomes better, fluctuation effects must be weaker. There are basically two reasons for this outcome. The first reason is that with increasing valency more counterions are condensed or localized inside the brush, and the overall counterion distribution becomes very inhomogeneous. Also, in a mixture of multi- and monovalent counterions, a small but significant fraction of monovalent counterions is outside the brush, whereas the multivalent ones are completely trapped inside the brush due to their strong binding to the chains. This is also illustrated in Fig. 4. The second reason for the weak fluctuation effects at high valency is caused by the fact that at the same time the brush also shrinks with increasing valency, inducing a compact counterion structure similar to a form factor of a spherical object. In particular, this is well observed for $q \geq 3$ in Fig. 13. This is in line with the results we obtained so far. We conclude that fluctuation effects become weaker with increased valency of the counterions. This fact is used in our mean-field approach described in Sec. III and explains why it is able to describe the brush collapses observed in experiments and simulation.

V. CONCLUSIONS

In conclusion, we demonstrated that the experimentally measured brush collapse can be well described by a mean-field model. The model also describes our simulation results regarding the collapse of a single SPB in the presence of a mixture of monovalent counterions and counterions with valencies between 2 and 4. The physical reasons are twofold. One is the decreased osmotic pressure because there are fewer ions inside the brush if q monovalent counterions are essentially replaced by one counterion of valency q. In the presence of added salt the mechanism of ion exchange is controlled by the Donnan equilibrium. The second reason for the collapse results from the strong binding of the ions to the polyelectrolyte chains. In our simulation study we investigated this aspect in detail. It was confirmed that indeed the multivalent counterions, in particular at valencies above 2, are strongly correlated with the chains. Their translational degree of freedom, expressed by the mobility, is significantly reduced. As a consequence of the strong ion chain correlation, the osmotic activity of these ions is negligible. This was a central assumption in the mean-field model and is confirmed now by these findings. In contrast, the monovalent counterions, and partially also the divalent ones, prevent the brush from a full collapse. A further relevant aspect for our considerations is the importance of counterion fluctuations. In fact, the counterion fluctuations have been shown to become weaker as their valency is increased. Again, the strong binding prevents fluctuations and, hence, their influence is negligible.

From the analysis of the virial contributions to the osmotic pressure we note that for ion fractions $\Phi \gtrsim 1$ the osmotic pressure becomes negative, although the absolute values are small. We found that electrostatic contributions are outmatched by short-ranged excluded volume contributions of the counterions. The negative value of the total osmotic pressure at high counterion valency stems from chain contributions. This points to additional attractions that could fortify the collapse and that could explain the experimentally observed coagulation of the SPBs at ionic strengths above 0.006 M. However, we stress that the observed collapse of the experimental and of the model SPBs is mainly driven by the reduction of the osmotic pressure inside the brush, and is therefore primarily of entropic nature.

ACKNOWLEDGMENTS

The authors thank C. N. Likos and J. Davis for helpful discussions. We wish to acknowledge the financial support of the Deutsche Forschungsgemeinschaft (DFG), Sonderforschungsbereich 481, Bayreuth, from the DFG research group "Polyelectrolytes," and of the Fonds der Chemischen Industrie. A.J. gratefully acknowledges financial support by the DFG. The authors also acknowledge financial support by the European Community, Marie Curie Research and Training Network POLYAMPHI.

APPENDIX: DONNAN EQUILIBRIUM OF A TWO-COMPONENT SPB-ION SOLUTION

The SPB is dissolved in a mixture of monovalent and multivalent salt solution. The equilibrium condition for the concentrations of each ion type $(+, q+, -)$ inside and outside the brush is determined by the requirement that the Gibbs free energy $G(N_x, p, T)$ $(x = +, q+, -)$ possess a minimum, i.e., $dG = \Sigma_x(\mu_x^i dN_x^i + \mu_x^o dN_x^o) = 0$; $\mu_x^{i/o}$ is the chemical potential of each component inside (i) and outside (o) the brush; $N_x^{i/o}$ is the number of ion species x inside and outside the brush. In addition, the neutralization condition holds inside and outside the brush: $\Sigma_x q_x dN_x^i = 0$ and $\Sigma_x q_x dN_x^o = 0$, respectively, with q_x being the valency of each ion species. Since the total number of each ion species in the system is constant, we also require $dN_x^i + dN_x^o = 0$. Combining these conditions yields

$$\mu_+^i - \mu_+^o = \frac{\mu_{q+}^i - \mu_{q+}^o}{q}, \tag{A1}$$

$$\mu_-^i - \mu_-^o = -\frac{\mu_{q+}^i - \mu_{q+}^o}{q}. \tag{A2}$$

Although both sides in both equations vanish at equilibrium, we can extract important information from these relations. For the sake of simplicity we assume that outside the brush the ions possess only an ideal contribution to the chemical potential: $\mu_x^o = kT \ln(c_x^o)$. This is justified since most experimental SPBs are measured in dilute solutions. However, inside the brush there are also other terms that contribute to the

chemical potential, such as the electrostatic interactions between ions. It can be shown in a few steps that these contributions cancel in a mean-field approach as long as all ion distributions inside the brush possess the same density profile regarding their functional form. This is due to the neutralization condition. In our present case, we assumed that all ions are homogeneously distributed inside the brush. The remaining parts are the ideal gas terms $\mu_x^i = kT \ln(c_x^i)$. Using μ_x^i and μ_x^o in Eqs. (A1) and (A2) we readily obtain the Donnan equation (4).

[1] X. Guo and M. Ballauff, Langmuir **16**, 8719 (2000).
[2] X. Guo and M. Ballauff, Phys. Rev. E **64**, 051406 (2001).
[3] Y. Mei and M. Ballauff, Eur. Phys. J. E **16**, 341 (2005).
[4] M. Ballauff and O. Borisov, Curr. Opin. Colloid Interface Sci. **11**, 316 (2006).
[5] P. Pincus, Macromolecules **24**, 2912 (1991).
[6] O. V. Borisov, T. M. Birshtein, and E. B. Zhulina, J. Phys. II **1**, 521 (1991).
[7] H. Ahrens, S. Förster, and C. A. Helm, Phys. Rev. Lett. **81**, 4172 (1998).
[8] M. Biesalski, J. Rühe, and D. Johannsmann, J. Chem. Phys. **111**, 7029 (1999).
[9] E. P. K. Currie, A. B. Sieval, M. Avena, H. Zuilhof, E. J. R. Sudhölter, and M. A. Cohen Stuart, Langmuir **15**, 7116 (1999).
[10] S. W. An, P. N. Thirtle, R. K. Thomas, F. L. Baines, N. C. Billingsham, S. P. Armes, and J. Penfold, Macromolecules **32**, 2731 (1999).
[11] Y. Tran, P. Auroy, and L.-T. Lee, Macromolecules **32**, 8952 (1999).
[12] E. P. K. Currie, A. B. Sieval, G. J. Fleer, and M. A. Cohen Stuart, Langmuir **15**, 7116 (1999).
[13] M. N. Tamashiro, E. Hernández-Zapata, P. A. Schorr, M. Balastre, M. Tirrell, and P. Pincus, J. Chem. Phys. **115**, 1960 (2001).
[14] Y. Tran and P. Auroy, Eur. Phys. J. E **5**, 65 (2001).
[15] M. Biesalski, D. Johannsmann, and J. Rühe, J. Chem. Phys. **117**, 4988 (2002).
[16] M. Biesalski, D. Johannsmann, and J. Rühe, J. Chem. Phys. **120**, 8807 (2004).
[17] B. Das, X. Guo, and M. Ballauff, Prog. Colloid Polym. Sci. **121**, 34 (2003).
[18] D. Bendejacq, V. Ponsinet, and M. Joanicot, Eur. Phys. J. E **13**, 3 (2004).
[19] F. von Goeler and M. Muthukumar, Macromolecules **28**, 6608 (1995).
[20] F. von Goeler and M. Muthukumar, J. Chem. Phys. **105**, 11335 (1996).
[21] V. A. Pryamitsyn, F. A. M. Leermakers, G. J. Fleer, and E. B. Zhulina, Macromolecules **29**, 8260 (1996).
[22] F. S. Csajka and C. Seidel, Macromolecules **33**, 2728 (2000).
[23] P. Gong, J. Genzer, and I. Szleifer, Phys. Rev. Lett. **98**, 018302 (2007).
[24] E. B. Zhulina, O. V. Borisov, and T. M. Birshtein, Macromolecules **32**, 8189 (1999).
[25] C. D. Santangelo and A. W. C. Lau, Eur. Phys. J. E **13**, 335 (2004).
[26] Y. Mei, K. Lauterbach, M. Hoffmann, O. V. Borisov, M. Ballauff, and A. Jusufi, Phys. Rev. Lett. **97**, 158301 (2006).
[27] A. Ishikubo, J. W. Mays, M. Tirrell, and A. C. S. Div, Polym. Prepr. (Am. Chem. Soc. Div. Polym. Chem. **46**, 27 (2005).
[28] S. Alexander, J. Physiol. (Paris 1946–1992) **38**, 983 (1977).
[29] P. G. de Gennes, Macromolecules **13**, 1069 (1980).
[30] G. Romet-Lemonne, J. Daillant, P. Guenoun, J. Yang, and J. W. Mays, Phys. Rev. Lett. **93**, 148301 (2004).
[31] H. Ahrens, S. Förster, C. A. Helm, N. Arun Kumar, A. Naji, R. R. Netz, and C. Seidel, J. Phys. Chem. B **12**, 108 (2004).
[32] A. Jusufi, J. Chem. Phys. **124**, 044908 (2006).
[33] A. Jusufi, C. N. Likos, and H. Löwen, J. Chem. Phys. **116**, 11011 (2002).
[34] J. Lekner, Physica A **176**, 485 (1991).
[35] R. Sperb, Mol. Simul. **13**, 189 (1994); **20**, 179 (1998).
[36] M. Murat and G. S. Grest, Macromolecules **22**, 4054 (1989).
[37] G. S. Grest, K. Kremer, S. T. Milner, and T. A. Witten, Macromolecules **22**, 1904 (1989).
[38] F. S. Csajka, R. R. Netz, C. Seidel, and J.-F. Joanny, Eur. Phys. J. E **4**, 505 (2001).
[39] A. Naji, R. R. Netz, and C. Seidel, Eur. Phys. J. E **12**, 223 (2003).
[40] M. P. Allen and D. J. Tildesley, *Computer Simulation of Liquids* (Clarendon, Oxford, 2004).
[41] D. Yin, Q. Yan, and J. J. de Pablo, J. Chem. Phys. **123**, 174909 (2005).
[42] C. G. Baumann, S. B. Smith, V. A. Bloomfield, and C. Bustamante, Proc. Natl. Acad. Sci. U.S.A. **94**, 6185 (1997).
[43] R. Golestanian, M. Kardar, and T. B. Liverpool, Phys. Rev. Lett. **82**, 4456 (1999).
[44] G. Ariel and D. Andelman, Phys. Rev. E **67**, 011805 (2003).
[45] Y. Hayashi, Europhys. Lett. **68**, 536 (2004).
[46] O. E. Philippova, T. Akitaya, I. R. Mullagaliev, A. R. Khokhlov, and K. Yoshikawa, Macromolecules **38**, 9359 (2005).
[47] J. P. Hansen and I. R. McDonald, *Theory of Simple Liquids*, 2nd ed. (Academic, London, 1986).
[48] I. O. Götze and C. N. Likos, J. Phys.: Condens. Matter **17**, S1777 (2005).